The Properties of Electrochemically-Grown Copper Sulfide Films

The Properties of Electrochemically-Grown Copper Sulfide Films

T. Martino,[1] J. Smith,[2] J. Chen,[1,z] Z. Qin,[1] J. J. Noël,[1,3,*] and D. W. Shoesmith[1,3,]**

[1]*Department of Chemistry, Western University, London, Ontario N6A 3K7, Canada*
[2]*Canadian Nuclear Laboratories, Chalk River, Ontario K0J 1J0, Canada*
[3]*Surface Science Western, London, Ontario N6A 5B7, Canada*

The electrochemical growth of copper sulfide films on copper has been studied voltammetrically and potentiostatically in 0.1 M sodium chloride solutions containing sulfide concentrations ranging from 10^{-4} M to 10^{-3} M. The properties of the films formed were investigated using electrochemical impedance spectroscopy. Film growth was observed to occur in two stages: the initial formation of a thin porous base layer at low potentials, followed by film restructuring leading to increased porosity and the deposition of an outer copper sulfide layer at more positive potentials. At more oxidizing potentials the overall film growth rate was determined by the properties of the outer deposit, not by the formation of a passive barrier layer at the Cu/film interface.
 [DOI: 10.1149/2.0321902jes]

Manuscript submitted September 13, 2018; revised manuscript received December 17, 2018. Published January 9, 2019.

Nuclear energy has proven to be a viable option as a reliable, inexpensive, and CO_2-neutral source of electrical energy. However, with these advantages comes the responsibility for the secure management of the spent nuclear fuel. One approach under study in many countries, including Sweden, Finland and Canada, is permanent disposal of the spent fuel in a deep geological repository (DGR). The spent fuel would be placed in containers fabricated with a cast iron or carbon steel inner vessel and an outer copper shell, designed to avoid both corrosion and mechanical failure. It is proposed that these containers be buried in crystalline rock, approximately 500 m below the surface, and the excavated boreholes be backfilled with bentonite clay.[1] In Sweden and Finland, the outer shell would be fabricated using P-deoxidized Cu, with a thickness of 50 mm.[2–4] Small additions of P (30 to 100 ppm) improve the creep properties, thereby limiting the probability for mechanical failure of the container after emplacement.[5] Although Cu is chosen for its resistance to corrosion in anoxic environments,[3–5] Scandinavian repositories are known to contain SH^-, produced in the groundwater as a consequence of sulfate-reducing bacteria and mineral dissolution processes.[6] This is potentially detrimental to the container, since SH^- can act as an oxidant for Cu. Previous studies have characterized the copper sulfide films grown both electrochemically[7–9] and under corrosion conditions in aqueous solutions containing SH^-.[6,10–14]

Corrosion studies have shown that the properties of the sulfide films formed over exposure periods up to 1691 h are governed by the sulfide concentration ($[SH^-]$). Film growth as chalcocite (Cu_2S) occurred at the film/electrolyte interface.[14] Under stagnant conditions in 5×10^{-4} M SH^- + 0.1 M NaCl solution, a parabolic growth law was observed, with growth controlled mainly by Cu^+ transport in the compact film.[6] However, at lower $[SH^-]$ a linear growth law was observed, leading to the development of a Cu_2S film with a cellular structure, whose growth was controlled predominantly by SH^- diffusion in solution. When the Cu_2S films were grown electrochemically for times ranging from 5 to 10 min,[7,8] their properties were found to be dependent not only on the $[SH^-]$ but also on $[Cl^-]$ and the transport flux of SH^- to the Cu surface (controlled using a rotating disc electrode (RDE)). The use of a RDE allows control of the mass transport of SH^- and aids in determining its role in the film growth process, albeit at fluxes well in excess of those anticipated in a DGR (10^{-6} mol · m^{-2} · a^{-1}).[15] At low $[SH^-]$, a thin, single-layer, porous film was formed, with a dual-layer film developing as the $[SH^-]$ was increased. For sufficiently high $[SH^-]$ ($\geq 10^{-3}$ M), the anodic current became almost independent of the transport flux and decreased at higher potentials (≥ -0.85 V/SCE), indicating at least partial passivation of the Cu surface.

Other authors have claimed that the film formed on Cu under electrochemical conditions in 2×10^{-4} M SH^- was passive in nature,[16–18] which ultimately led to Cl^--induced breakdown and pitting at very positive potentials. However, these claims were based on polarization curves recorded under stagnant conditions, while our results, recorded at a rotating disk electrode (RDE),[7] demonstrated that the current observed was due to film growth partially controlled by SH^- transport, a situation which precluded the possibility of passivation.[8] Additionally, the current increase observed at very positive potentials was shown to be due to the active anodic dissolution of Cu, accelerated by complexation with chloride to form soluble species, such as $CuCl_2^-$, at the base of pores within the porous, non-protective chalcocite layer,[8] not to the breakdown of a passive copper sulfide film.

These observations, however, conflict with claims,[16–18] based on EIS measurements and Mott-Schottky analyses, that film growth was controlled by the transport of Cu^+ vacancies within a passive film, with a diffusion coefficient in the range of 10^{-14} to 10^{-15} cm^2/s. These values, obtained for films ranging from ~0.1 μm to ~50 μm in thickness, are considerably lower than the diffusion coefficients measured for Cu^+ vacancies in various copper sulfides, which vary with the degree of non-stoichiometry, decreasing from $\sim 10^{-8}$ cm^2/s for chalcocite (Cu_2S) to 10^{-9} cm^2/s for djurleite ($Cu_{1.96}S$), to 10^{-10} to 10^{-11} cm^2/s for anilite ($Cu_{1.75}S$) and 10^{-12} cm^2/s for covellite (CuS).[19] Values, more consistent with these expectations, were measured in our corrosion experiments. For the compact film grown in a solution containing 5×10^{-4} M SH^-, a diffusion coefficient of 3.6×10^{-10} cm^2/s was obtained,[6] while for films grown at the lower $[SH^-]$ of 5×10^{-5} M, the diffusion coefficient evolved from 10^{-7} cm^2/s, consistent with SH^- transport within a porous chalcocite film, to 1.73×10^{-5} cm^2/s in agreement with the value measured for SH^- in bulk solution.[10] However, it is possible that diffusivities obtained for bulk electrodes may differ from those obtained for thin films. While some doubt exists over the analysis of Kong et al.,[17,18] since no attempt was made to eliminate solution transport effects, these observed differences in the measured diffusion coefficients for corrosion and electrochemical films could reflect a difference in the chemical nature of the films.

These large differences raise the question of whether the films grown electrochemically at potentials positive to the corrosion potential (E_{corr})[16–18] possess different properties to those grown at E_{corr}, i.e., at open circuit.[6,10] That this may be the case was suggested by the voltammetric experiments of Martino et al.,[7] which showed that, at high $[SH^-]$ ($\geq 10^{-3}$ M), an increase in current at small oxidizing potentials (defined by the difference, $E_{applied} - E_{corr}$) was followed by a major decrease to a subsequently potential-independent current, suggesting passivation. It was proposed that this film could be CuS, but no analytical supporting evidence was provided. The structure and properties of the sulfide films formed electrochemically were also investigated by Kong et al.,[17] but their claim that CuS was formed was

*Electrochemical Society Member.
**Electrochemical Society Fellow.
[z]E-mail: jchen496@uwo.ca

based on a misinterpretation of XPS spectra, which cannot be used to distinguish between Cu_2S and CuS. However, transmission electron microscopy (TEM) evidence has been published to show that the Cu_2S film which formed at low potentials was converted to a more passive CuS film as the potential was made more positive, although the potential at which this occurred was not defined.[20] These last results appear to support the tentative claims of Martino et al.[7]

The purpose of this paper is to clarify the nature of the sulfide film grown at potentials positive to E_{corr}, to determine whether the formation of a passive film is possible, and to demonstrate whether or not electrochemically grown films are representative of those formed at open circuit. Knowledge of the characteristics of the sulfide film expected on a nuclear fuel waste container is essential to determining whether or not localized corrosion, in the form of pitting, is a possible degradation mechanism.

Experimental

Electrochemical cell and instrumentation.—All electrochemical data were collected using a conventional three-electrode electrochemical glass cell. A Pt sheet rolled into a cylinder was used as the counter electrode and connected to external circuitry by a Pt wire. A saturated calomel electrode (SCE, 0.242 V/SHE) was used as the reference electrode in all experiments. The cell was housed inside a Faraday cage to reduce electrical noise from external sources. Cyclic voltammetry experiments were conducted using a rotating disc working electrode (RDE). The electrode rotation rate was controlled by a Pine Instrument Company Analytical Rotator Model AFA86 Serial 882. Electrochemical measurements were performed using either a computer-controlled Solartron 1287 potentiostat equipped with CorrWare software with a Solarton 1255B frequency response analyzer (FRA) with Zplot software for EIS data collection, or a Solartron Analytical Modulab running Modulab XM ECS software.

Copper composition and electrode preparation.—O-free, P-doped Cu, provided by the Swedish Nuclear Fuel & Waste Management Co. (SKB, Solna, Sweden), was machined into Cu disks. Ti rods were threaded into the back of the discs and the Cu was fixed in a polytetrafluoroethylene (PTFE) holder using an epoxy resin. Only a single flat Cu face, with a surface area of 0.785 cm^2, was exposed to solution. Prior to each experiment, the Cu electrode was ground with a sequence of SiC papers with grit sizes 1000, 1200, and 4000, and then polished to a mirror finish with Al_2O_3 suspensions with decreasing particle size (1 μm, 0.3 μm, and 0.05 μm). The electrode was then rinsed thoroughly with Type-1 water (resistivity: 18.2 MΩ · cm) to remove any polishing residue, and finally dried in a stream of ultrapure Ar gas.

Solution preparation.—Electrolytes were prepared with Type-1 water obtained from a Thermo Scientific Barnstead Nanopure 7143 water system. All water was sparged with high purity Ar gas (Praxair) for 1 h prior to the preparation of solutions. This was necessary to avoid sulfide oxidation prior to experiments. Solutions were made from reagent-grade sodium sulfide ($Na_2S \cdot 9H_2O$, 98.0% assay) and sodium chloride (NaCl, 99.0% assay) purchased from Sigma-Aldrich and Caledon Laboratory Chemicals, respectively. All solutions contained 0.1 M NaCl and Na_2S concentrations of 10^{-4} M, 2×10^{-4} M, 3×10^{-4} M, 4×10^{-4} M, 5×10^{-4} M and 10^{-3} M. To ensure the maintenance of an anoxic environment and minimize sulfide oxidation, solutions were Ar-sparged for a further 45 min before each experiment, with sparging continued throughout the experiment.

Electrochemical experiments.—Cyclic voltammetric (CV) experiments were performed using RDEs. Prior to applying a voltammetric scan to the electrode, it was cathodically cleaned at −1.5 V/SCE for 60 s to reduce air-formed oxides, and then at −1.15 V/SCE for a further 60 s to allow the detachment of any H_2 bubbles which may have formed due to H_2O reduction at the more negative potential. Voltammetric scans were then performed to various more positive potential limits at a scan rate of 2 mV/s and an electrode rotation rate of 8.3 Hz.

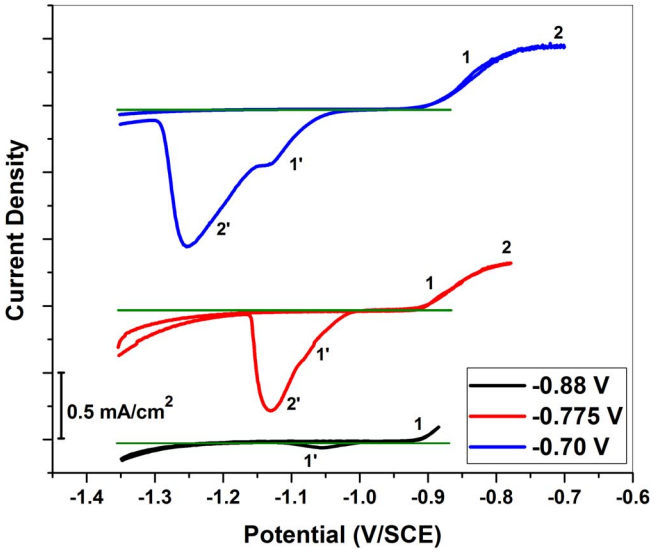

Figure 1. CVs recorded to various upper potential limits in a 0.1 M NaCl and 5×10^{-4} M Na_2S solution at an electrode rotation rate of 8.33 Hz. The green line denotes zero current density.

Prior to electrochemical impedance spectroscopy (EIS) measurements, films were grown for 2 h at a series of applied potentials, with the potential being increased in 10 mV increments from E_{corr}. At each applied potential, the current was allowed to achieve a steady-state value before an EIS spectrum was recorded. Spectra were recorded in the frequency range 10^5 Hz to 10^{-3} Hz using a sinusoidal potential perturbation of 10 mV amplitude superimposed on the applied potential. The self-consistency of the measured spectra was confirmed using the Kramers-Krönig transformation. Equivalent circuits were fit to data using ZView software (version 3.5a). Samples used for surface analyses were prepared by applying a constant anodic current for 2 h, rinsing with Type-1 water on removal from the electrochemical cell, and then finally drying with a stream of Ar gas.

Surface analysis.—Surface imaging was performed using a LEO (Zeiss) 1540XB FIB/SEM, equipped with an energy dispersive X-ray spectroscopy (EDX) analyzer to elucidate the elemental composition of the surface. Analyses were performed at the Western Nanofabrication Facility. Focused ion beam (FIB) cross sections were prepared using a Ga ion beam. The sample was not pre-coated before cutting.

Results and Discussion

Cyclic voltammetry.—CVs with the potential scanned to a series of positive limits, recorded on a RDE in a solution containing 5×10^{-4} M SH^-, Figure 1, exhibited two reduction peaks indicating the presence of a dual-layer film, as previously observed over a wide range of $[SH^-]$ and $[Cl^-]$.[7] When the upper potential limit of the CV was confined to −0.88 V/SCE, anodic oxidation (1) led to a single, shallow, reduction peak on the reverse scan (1'). When the scan was extended to −0.775 V/SCE, the anodic current approached a plateau (2) and a second reduction peak (2') was observed on the reverse scan in addition to the shoulder attributed to the film grown at lower potentials (1'). The charge associated with reduction peak 2' was considerably larger than that reduced at 1'. The maintenance of the anodic current on the negative-going scan indicated that the film formed on the positive-going scan did not passivate the electrode surface. The film formed at low potentials (1) appeared not to grow significantly on extending the upper potential limit, with its reduction generating only a shallow shoulder (1') on the reverse scan. This behavior was confirmed when the positive-going scan was extended further, to a limit of

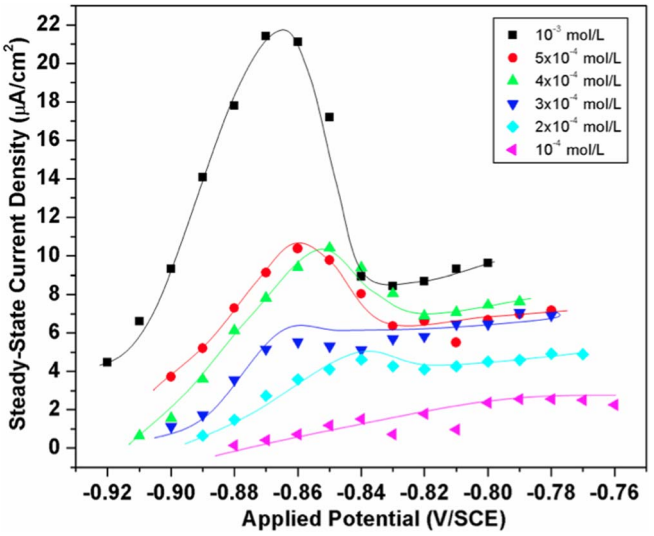

Figure 2. Steady-state current densities obtained after potentiostatic oxidation for 2 h in 0.1 M NaCl solutions containing various sulfide concentrations.

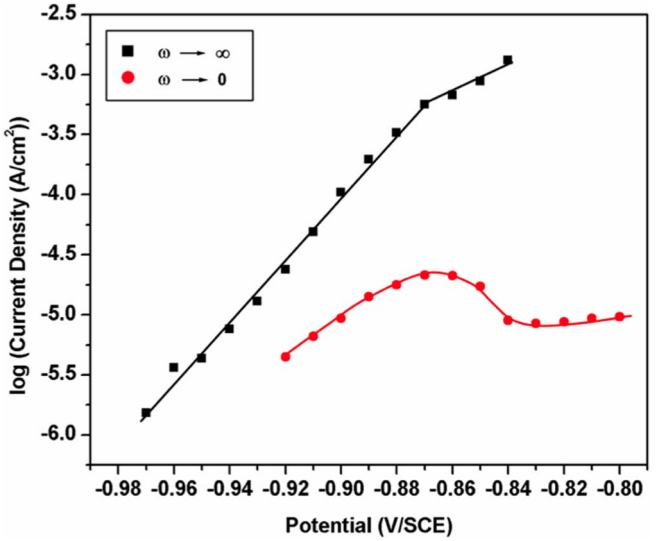

Figure 3. Current – potential relationships determined in a 0.1 M NaCl + 10^{-3} M Na_2S solution under stagnant ($\omega = 0$) and mass transport corrected ($\omega \rightarrow \infty$) conditions.

−0.70 V/SCE, when the anodic current achieved a plateau leading to an enhanced growth of peaks 2/2' but only a marginal further growth of peaks 1/1'.

Consistent with previous observations,[7] based on experiments conducted over a wide range of [SH^-] (5×10^{-5} M to 2×10^{-3} M), these CVs suggest that Cu_2S film growth occurred as two layers, with the initially grown film (peaks 1/1') achieving only a limited thickness, with most of the film growth occurring as a much thicker outer layer (peaks 2/2'). The reproducibility of the anodic current on the positive-going and negative-going scans showed that passivation did not occur at the mass-transport rate used in these experiments. Integration of the anodic and cathodic current sections of the CVs showed that effectively all the anodic charge injected on the forward and reverse scans was recovered by reduction of the films on the reverse scan. This confirmed that the film that was anodically grown on the positive-going potential scan was sufficiently porous to allow film growth to continue on the negative-going scan.[7] Similar non-passive behavior was observed for all [SH^-] lower than 5×10^{-4} M in solutions with [Cl^-] in the range 0.1 to 5.0 M.

Potentiostatic film formation.—Figure 2 shows steady-state polarization curves measured at a series of constant potentials on static electrodes in solutions containing various [SH^-]. In these experiments, steady-state current values were rapidly established (between 2 and 40 s). No tendency to decrease with time, indicating the development of a passive barrier layer, was observed. At low [SH^-] the current rose with increasing potential to a steady-state value. As the [SH^-] was increased, the current increased to a peak value before decreasing to a lower current plateau. This feature became clearly defined for [SH^-] $\geq 3 \times 10^{-4}$ M. However, as demonstrated in the CVs (Figure 1), anodic charge (Q_A) was consumed by Cu_2S film formation (equal to cathodic charge, Q_C). For the CV scanned to an upper limit of −0.7 V/SCE, the Q_A:Q_C was 1.1, which slightly deviated from unity due to the cathodic peak not being completely resolved before H_2O reduction occurred. Thus, the current peak shown in Figure 2 cannot be attributed to a standard transition from active metal dissolution to a film-covered passive state. In addition, the observations that negligible dissolution was observed, and that the increase in current with [SH^-] observed in the plateau region of the polarization curves (i.e., for potentials $\geq$ −0.83 V/SCE) only contributed to further film growth, are not consistent with the formation of a passive state. The only credible alternative is that the transition reflects a change in the properties of the Cu_2S film formed on the Cu surface.

Experiments repeated at a RDE yielded an increase in anodic current over those performed with a static electrode, which confirmed that the currents plotted in Figure 2 were at least partially controlled by SH^- transport. Figure 3 shows a comparison between transport-corrected currents (obtained using a Koutecky-Levich extrapolation) and the currents measured at a static electrode for [SH^-] = 10^{-3} M. While the current peak was eliminated by electrode rotation, a noticeable change in the potential dependence of the anodic film growth rate was observed in the potential range within which the current measured on static electrodes decreased. Previously, this decrease in anodic film growth rate was attributed to a two-step process,[21]

$$Cu + SH^- \rightleftharpoons Cu(SH)_{ads} + e^- \quad [1]$$

$$Cu + Cu(SH)_{ads} + SH^- \rightarrow Cu_2S + H_2S + e^- \quad [2]$$

It was proposed[21] that, at low potentials at a RDE, Reaction 1 approaches equilibrium but becomes totally irreversible and rate-controlling at high potentials, a change in kinetics that would account for the decrease in slope. However, the alternative explanation that this change in slope could be attributed to the formation of a CuS layer cannot be dismissed, since, at higher [SH^-], a current decrease was observed even at RDEs.[7]

SEM micrographs.—SEM images of FIB-cut cross sections are shown for the films grown at −0.76 V/SCE in the 10^{-4} M SH^- solution, and at −0.80 V/SCE in the 10^{-3} M SH^- solution in Figure 4. At the lower [SH^-], Figure 4a, the film was clearly porous leading to a roughened, but not pitted Cu surface. Since a thin passive barrier layer would form rapidly via the transport of microscopic defects through the growing film, it would be expected to lead to the uniform coverage of a relatively un-corroded (i.e., un-roughened) surface. At the higher [SH^-], Figure 4b, the Cu_2S layer was considerably thicker, as expected since a much larger charge was consumed in growing the film than at the lower [SH^-]. In addition, at the higher [SH^-] two distinct layers were present, an extremely porous base layer with an approximate thickness of 200 nm and a much thicker, more compact but still porous, outer layer. Figure 4c shows an SEM micrograph of the surface of the outer deposit grown at the higher [SH^-] confirming the distribution of pores. The observation of a thin inner layer and a thick outer deposit was consistent with the observation of two distinct layers seen as reduction processes (1' and 2') in the CV scans, Figure 1. The presence of a porous inner layer indicated the attempted, but unsuccessful, formation of a protective barrier layer.

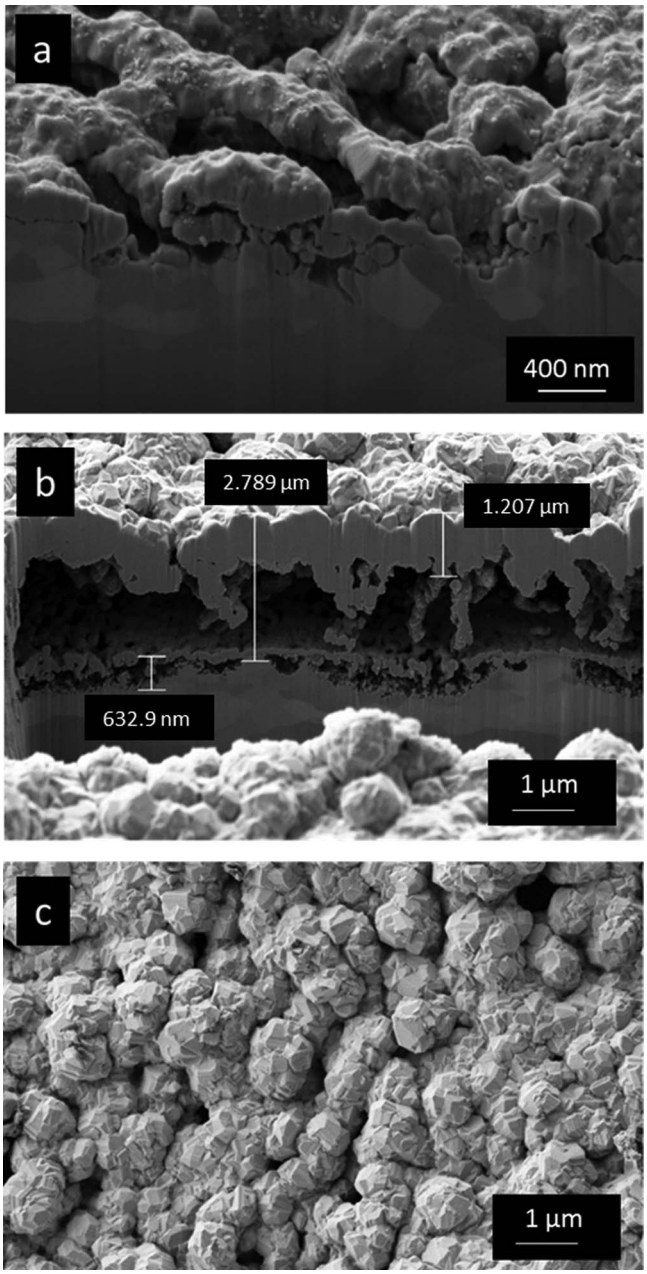

Figure 4. FIB-cut cross sections of films grown at (a) −0.76 V/SCE in a 10^{-4} M Na_2S solution, and (b) −0.80 V/SCE in a 10^{-3} M Na_2S solution. (c) An SEM micrograph of the surface of the film grown in the 10^{-3} M Na_2S solution.

The separation of the base layer from the Cu substrate, possibly during extraction of the specimen from the electrochemical cell and drying, confirmed that the corroded Cu surface was roughened but not pitted. The origin of the very large void space between the porous base layer and the outer deposit was uncertain but most likely due to the stresses developed at the corroding interface as the thick, porous layer grew.

Electrochemical impedance measurements.—*Low sulfide concentrations.*—Figure 5 shows that the EIS spectra recorded in the most dilute solution ($[SH^-] = 10^{-4}$ M) evolved as the potential was increased. At low potentials (−0.88 V/SCE and −0.87 V/SCE), two ill-defined responses were observed, marked 1 and 2 on the phase angle (θ) plot, Figure 5a. As the potential was increased (−0.86 V/SCE to −0.82 V/SCE), and the steady-state current in the polarization curve started to increase (Figure 2), the response at $\sim 10^{-1}$ Hz (2 in Figure 5a) became less distinct, and an additional low frequency response (3 in Figure 5a) was observed. Increasing the potential to values in the plateau region of the polarization curve (−0.81 V/SCE to −0.76 V/SCE, Figure 2)) led to a shift of the high frequency response (1 in Figure 5a) to even higher frequencies (~50 Hz) and the development of an additional low frequency response (4 in Figure 5a), accompanied by an increase in the impedance at the low frequency limit by approximately a factor of 10, Figure 5b.

A number of electrical equivalent circuits, Figure 6, were used to analyze the EIS spectra depending on the applied potential. Fits of the equivalent circuit in Figure 6a to EIS spectra recorded at low potentials (−0.88 V/SCE to −0.87 V/SCE), on the rising section of the polarization curve (Figure 2), are shown in Figure 7. The high frequency response (1 in Figure 5a) was attributed to the interfacial charge transfer process (R_{int}/CPE_{int}) occurring at the base of pores in the anodically-formed Cu_2S layer. Since this interfacial process involved surface-adsorbed species (Reaction 1), R_{int}/CPE_{int} included contributions from both charge transfer and the polarization of the surface-adsorbed species. No attempt was made to separate these contributions since the EIS spectra were insufficiently defined to merit it. The lower frequency response (2 in Figure 5a) was attributed to the properties of the porous layer (R_{pore}/CPE_{film}). Since this Cu_2S film was electrically conductive,[6] CPE_{film} will be a combination of the double layer capacitance, the capacitance associated with surface-adsorbed species involved in the film growth process, and possibly a contribution from the film itself.[6]

The equivalent circuit shown in Figure 6b, which includes a Warburg impedance (W_{SH}), was fit to the EIS spectra recorded at more positive potentials with a low frequency response (3 in Figure 5a), indicating a contribution from transport processes within pores in the surface film. Examples of fits of this circuit to the data are shown in Figure 8. The need for a Warburg impedance element was consistent with the electrode rotation rate dependence of the current demonstrated in Figure 3. Examples of fits of the equivalent circuit shown in Figure 6c to EIS spectra recorded at potentials in the plateau region of the polarization curve are shown in Figure 9. The additional time constant (4 in Figure 5a) is attributed to the resistance (R_{dep}) and capacitance (CPE_{dep}) of an outer layer deposit.

The assignment of the two CPE-R circuit components (R_{int}/CPE_{int} and R_{dep}/CPE_{dep}) in Figure 6c was based on the clear evidence of the formation of a porous deposit and the electrochemical evidence, Figure 2 and Figure 4, that the unlimited supply of SH^- at higher potentials led to enhanced film growth in the form of a thick outer deposited layer not the re-enforcement of a thin barrier layer. Since the interfacial reaction between Cu and SH^- is very fast, as indicated by the high currents recorded for transport-corrected conditions (Figure 3), we represented it by the high frequency response. Also, since there is a coincidence between the increasing importance of the low frequency response (4 in Figure 5) and the accumulation of the deposited film, we attribute this response to this deposition process.

In all these fits, and those described below, constant phase elements (CPEs) rather than capacitances were required to fit the equivalent circuits. The impedance, Z(ω), of the CPE can be defined by the following relationship:[22]

$$Z(\omega) = \frac{1}{Q(j\omega)^{\alpha}} \qquad [3]$$

where Q is the CPE parameter, j the imaginary unit (where $j^2 = -1$), ω the frequency, and α the exponent. When $\alpha = 1$ the CPE represents a true capacitor. However, attempts to calculate capacitances from the measured CPEs using the Mansfeld procedure[23] yielded unreasonable values.

The values of R_{int}, R_{pore} and R_{dep} obtained from fits to spectra at $[SH^-] = 10^{-4}$ M are plotted in Figure 10. In the potential range over which the current increased with potential in the polarization curve (up to −0.82 V/SCE (Figure 2)), the value of R_{int} changed only marginally, while R_{pore} decreased by approximately an order of magnitude. This decrease in R_{pore} was accompanied by the appearance of the Warburg

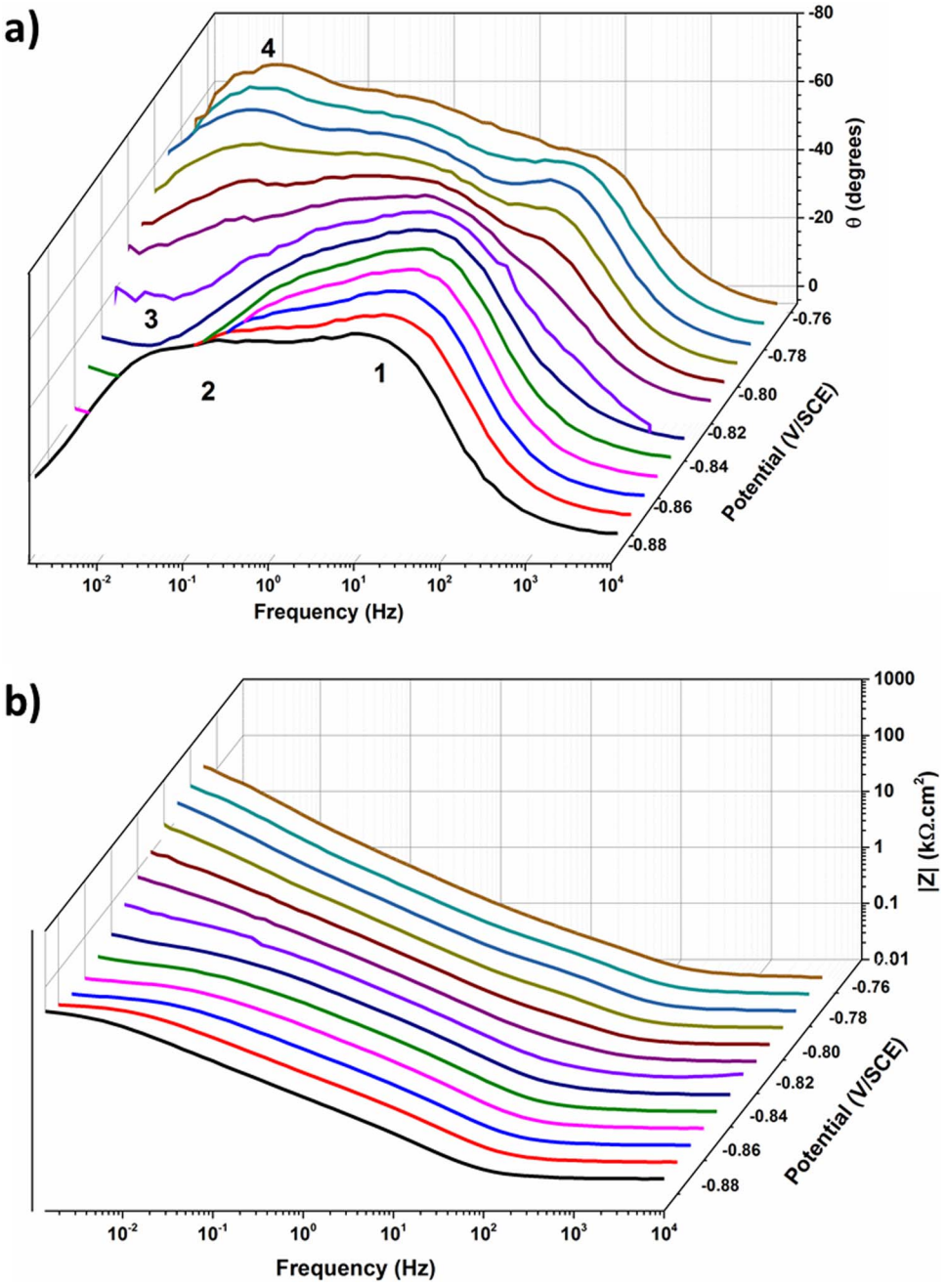

Figure 5. EIS spectra obtained after potentiostatic oxidation in a 0.1 M NaCl + 10^{-4} M Na_2S solution for 2 h: (a) phase angle (θ); (b) impedance modulus |Z|.

response at low frequencies (Figure 5). The interfacial resistance (R_{int}) at the base of pores would be expected to have decreased as the rate of the anodic reaction increased at more positive potentials. Its constancy can be attributed to the counterbalancing influence of film thickening leading to SH^- depletion at the Cu surface at the base of pores, as indicated in the spectra by the need to account for SH^- diffusion within the pores with a Warburg impedance, and the acceleration of the interfacial oxidation process as the potential was increased.

For potentials of −0.80 V/SCE and higher, both R_{int} and R_{pore} decreased markedly, indicating an increase in the rate of the interfacial reaction within a more porous film. This increased porosity facilitated the transport of Cu^+ to the film/electrolyte interface, leading to the formation of the outer sulfide deposit, with the large values of R_{dep} indicating that it was the accumulation of this deposit which controlled the overall rate of film growth at this [SH^-] on static electrodes. These results were consistent with the behavior observed in the CVs, Figure 1, in which the initially formed film (peaks 1/1') rapidly became more porous and were subsequently bypassed by the growth of the second layer (peaks 2/2').

At the highest potentials applied (−0.77 V/SCE and −0.76 V/SCE), R_{pore} appears to have increased again. This could have been due to the partial closing of porosity by deposition of Cu_2S within the pores, as illustrated in Figure 6c, making it difficult to deconvolute the resistances of the pore and the deposit when fitting the spectra. Additionally, it is possible, and indeed probable, that the overall film growth process remained diffusion-controlled by SH^- transport through the accumulating outer deposit, with this contribution incorporated into the value of R_{pore}.

Intermediate sulfide concentrations.—Similar EIS spectra were obtained for [SH^-] up to 3 × 10^{-4} M, the first concentration above

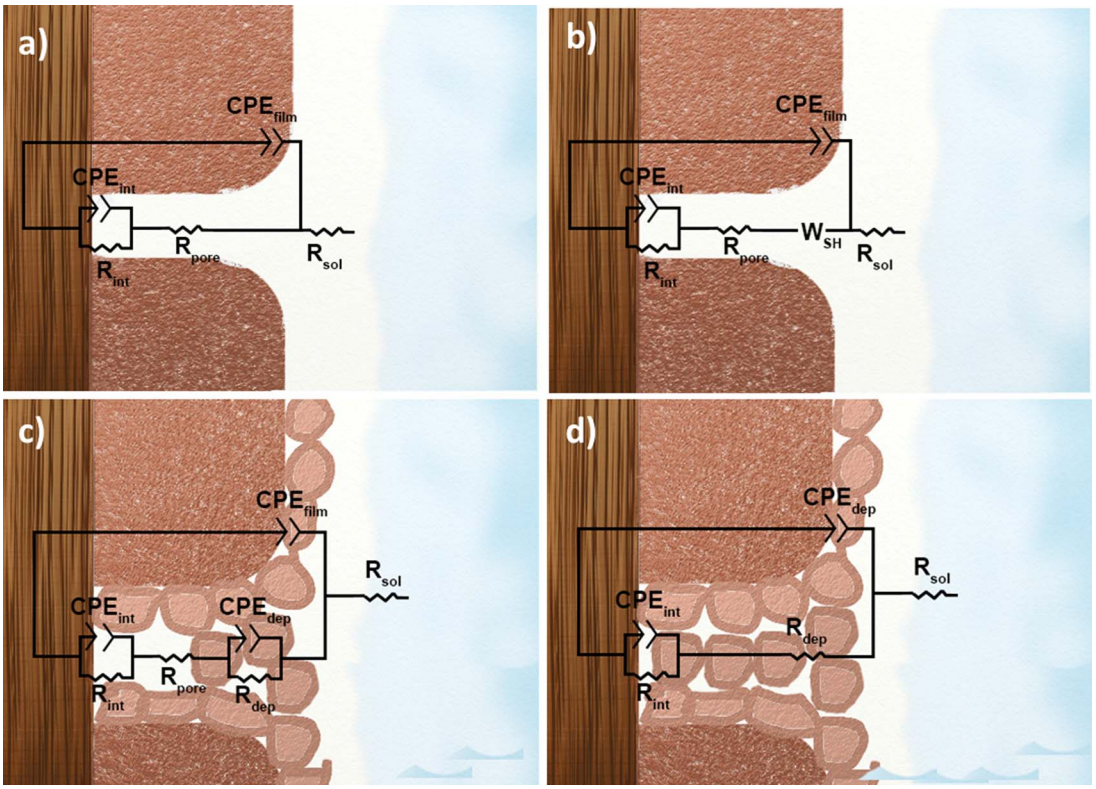

Figure 6. Equivalent circuits used to model EIS spectra recorded at various [SH^-]. The individual elements are defined in the text.

which the current peak became observable in the polarization curve, Figure 2. The resistance values obtained by fitting the equivalent circuits shown in Figures 6b and 6c to the spectra obtained in a solution containing 3×10^{-4} M SH^- are plotted in Figure 11. A decrease in R_{int} with increasing potential, similar to that observed at the lower concentration, was observed, although the decrease from the initially higher value to the eventually lower value occurred over a wider potential range (−0.88 V/SCE to −0.84 V/SCE) in this case. This change coincided with the shift from a current which increased with potential to one which was almost independent of potential, Figure 2 (−0.82 V/SCE to −0.8 V/SCE). However, in contrast to the behavior observed at the lower [SH^-], R_{pore}, which initially started to decline with increasing potential, did not undergo a distinct transition to a lower value over the same potential range (−0.88 V/SCE to −0.84 V/SCE). This could be attributed to the more rapid accumulation of the outer deposit within the developing pores at this higher [SH^-]. At higher potentials, R_{pore} and R_{dep} exhibited both similar values and identical increases with increasing potential. This coincidence suggests that these resistances were not very distinct in the EIS fitting procedure. The lower R_{int} and $R_{pore} + R_{dep}$ values at this concentration (compared to these values at the lower [SH^-]) were consistent with the larger currents measured in the polarization curves (Figure 2 at these high potentials) and indicated that, despite the more rapid formation of the outer deposit, the anodic film growth rate was

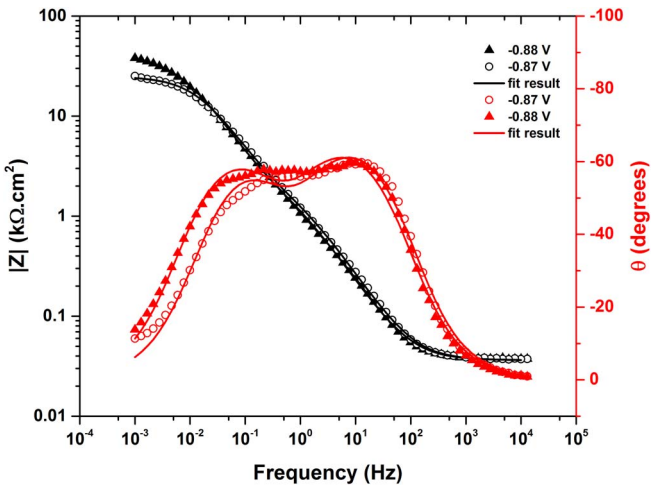

Figure 7. EIS spectra recorded at small positive potentials after potentiostatic oxidation for 2 h in a 0.1 M NaCl + 10^{-4} M Na_2S solution. EIS data are shown as symbols and the equivalent circuits fit as solid curves.

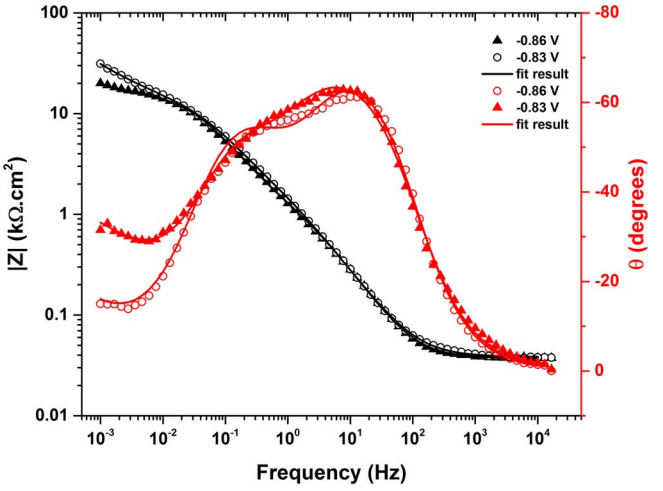

Figure 8. EIS spectra recorded at intermediate positive potentials after potentiostatic oxidation for 2 h in a 0.1 M NaCl + 10^{-4} M Na_2S solution. EIS data are shown as symbols and the equivalent circuit fits as solid curves.

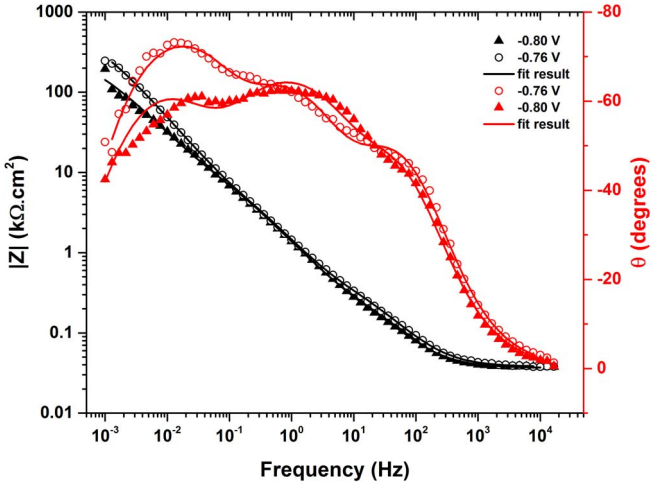

Figure 9. EIS spectra at large positive potentials after potentiostatic oxidation for 2 h in a 0.1 M NaCl + 10^{-4} M Na_2S solution. EIS data are shown as symbols and the equivalent circuit fits as solid curves.

higher. For this to have occurred, the transport of SH^- through the deposit to the Cu surface must have been maintained.

High sulfide concentrations.—For $[SH^-] \geq 4 \times 10^{-4}$ M, when the current peak was clearly visible in the polarization curves (Figure 2), the EIS spectra, shown for $[SH^-] = 5 \times 10^{-4}$ M in Figure 12, exhibited behavior similar to, but better-defined, than that observed at the lower $[SH^-]$. The high and intermediate frequency responses, in conjunction with the Warburg response, observed at low potentials confirmed that the initially formed film was porous. As the potential was made more positive, and the current in the polarization curve increased (−0.92 V/SCE to −0.86 V/SCE), the increased prominence of the low frequency Warburg response confirmed the increasing importance of SH^- transport within the porous film to the film growth process. At higher potentials, the disappearance of the Warburg impedance accompanied by the increased impedance at low frequencies is consistent with the decrease in current in the polarization curve (Figure 2), yielding firm evidence that this decrease in current could be attributed to the formation of the outer layer deposit.

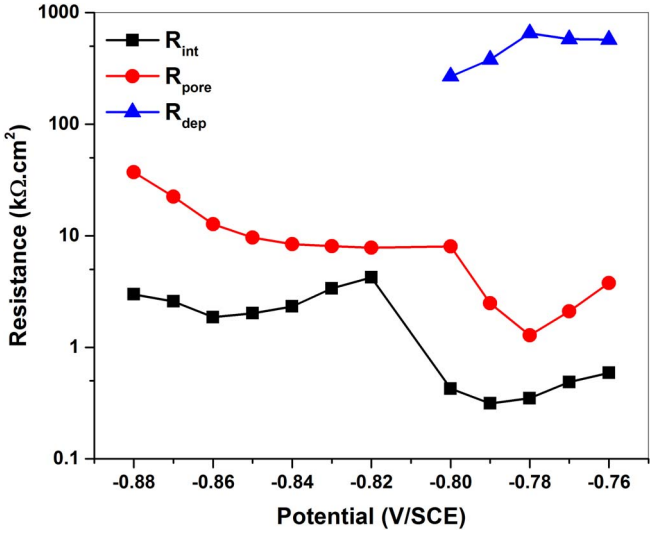

Figure 10. Resistance values obtained by fitting equivalent circuits in Figures 6a (−0.88 and −0.87 V/SCE), 6b (−0.86 to −0.82 V/SCE) and 6c (−0.80 to −0.76 V/SCE) to EIS spectra recorded in a 0.1 M NaCl + 10^{-4} M Na_2S solution.

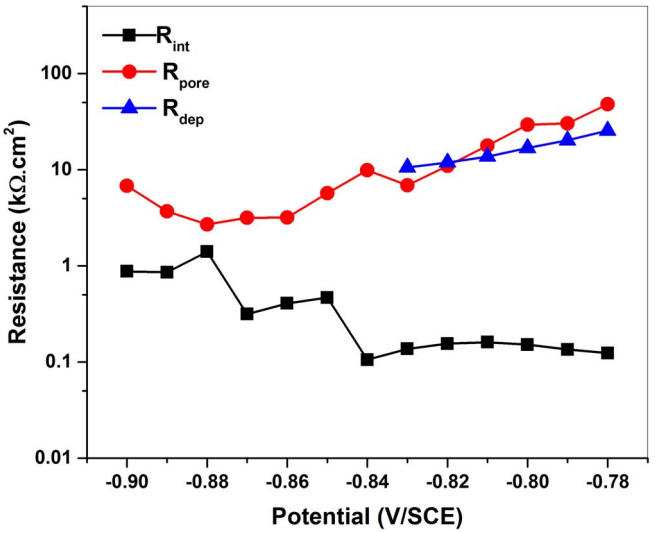

Figure 11. Resistance values obtained by fitting equivalent circuits in Figures 6b (−0.90 to −0.84 V/SCE) and 6c (−0.83 to −0.78 V/SCE) to EIS spectra recorded in a 0.1 M NaCl + 3 × 10^{-4} M Na_2S solution.

For low potentials (in the range within which the current increased with potential, Figure 2) the equivalent circuit shown in Figure 6b was fit to the spectra. At higher potentials (within the current plateau region (Figure 2)) the circuit in Figure 6d was used. The two circuits are the same except for the removal of the Warburg impedance in the second circuit and the redefinition of the pore resistance (R_{pore}) as the resistance of the outer layer deposit (R_{dep}). A contribution from the transport of SH^- within the deposit-filled pores remained, since a significant film growth current persisted (Figure 2), but became unobservable.

The redefinition of R_{pore} as R_{dep} acknowledges that deposition of the outer layer within the pores led to their blockage at high $[SH^-]$. To confirm this transition between the two circuits both equivalent circuits (Figures 6b and 6d) were fit to the spectrum recorded at −0.84 V/SCE. The extracted values for R_{ct} and R_{pore} (R_{dep}) coincide, Figure 13, confirming that the redefinition is appropriate.

In the equivalent circuit in Figure 6d, the CPE_{film} was redefined as CPE_{dep}. This acknowledged that, while the capacitive properties of the outer deposit dominated the impedance response, the porous base layer, shown to be present in Figure 4b, remained a source of capacitive charging of the interface. If a contribution from the base layer was ignored and the CPE_{dep} placed in parallel with R_{dep} in the equivalent circuit, the values of R_{int}, R_{dep} and R_{sol} were indistinguishable from those derived by fitting to the equivalent circuit in Figure 6c. This confirmed that the properties of the two layers became indistinguishable with the properties of the deposited outer layer dominating the interfacial behavior.

Despite the deposition of this layer the rate of the interfacial anodic reaction remained high, as indicated by the low value of R_{int}, which was constant over the full potential range investigated, Figure 13. For this to be the case, the rate of formation of Cu^+ at the Cu/Cu_2S interface must have remained effectively constant at this $[SH^-]$ despite the decrease in activation energy for the oxidation reaction and the on-going accumulation of the outer layer deposit. If the increased impedance was due to the formation of a passive layer, this interfacial rate would have been expected to decrease with increasing potential. As noted for the behavior at lower $[SH^-]$, the decrease in R_{pore} over the potential range within which the current increased in the polarization curve confirmed that the more rapid film growth sustained at this higher $[SH^-]$ was accompanied by a pore opening process in the initially-formed layer.

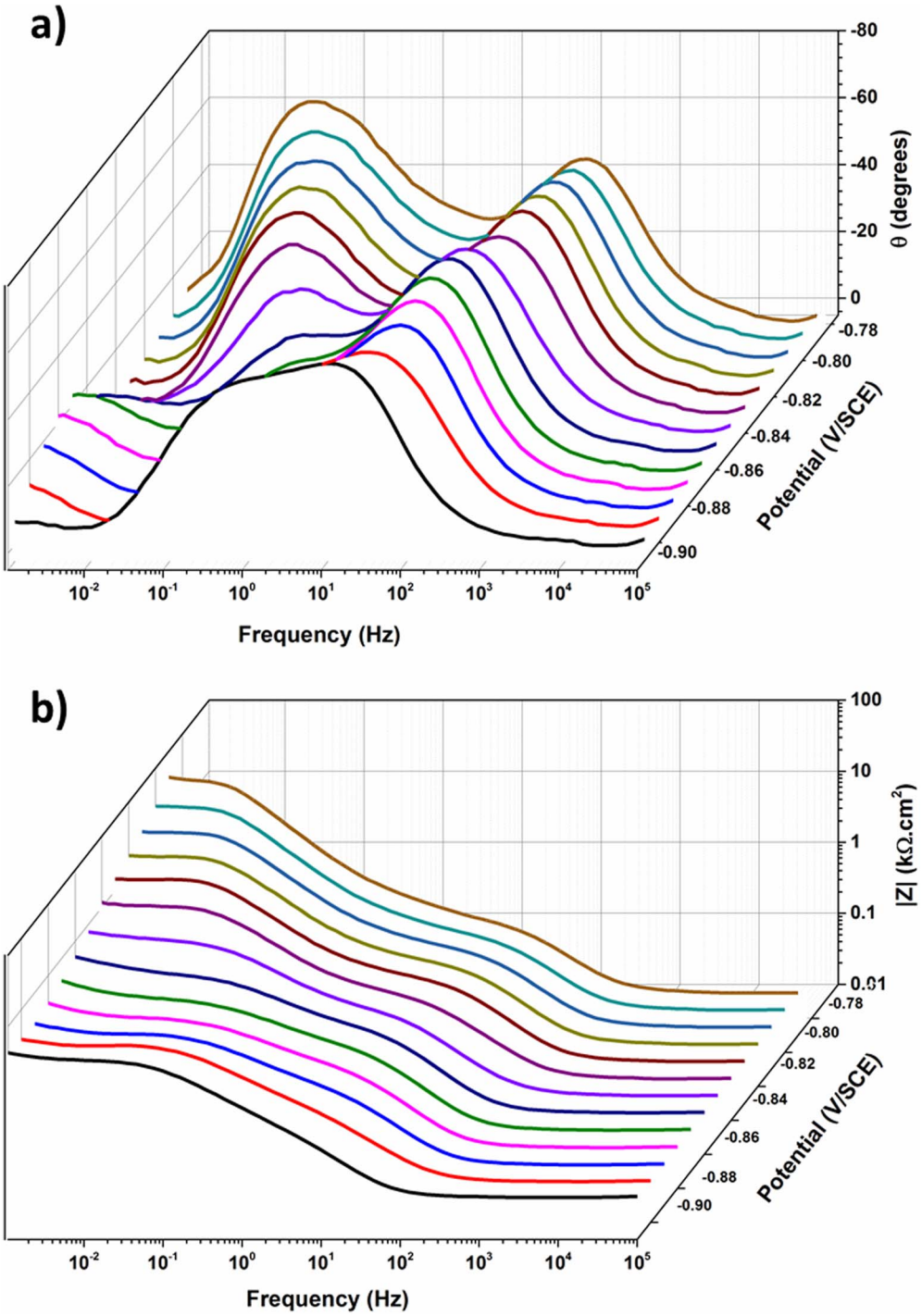

Figure 12. EIS spectra obtained after potentiostatic oxidation in a 0.1 M NaCl + 5 × 10^{-4} M Na_2S solution for 2 h: (a) phase angle (θ); (b) impedance modulus |Z|.

Influence of transport processes on film growth.—A critical feature of this analysis is the claim that the initial sulfide film formed was porous, allowing film growth to be sustained by SH^- transport within the porous structure to the Cu surface at the base of the pores. The Warburg impedance element (W_{SH}), representative of sulfide transport, is defined by,[22]

$$W(\omega) = \frac{\sqrt{2}\sigma_W}{\sqrt{j\omega}} \qquad [4]$$

where σ_W is the Warburg coefficient, which can be approximated by the relationship,

$$\sigma_W = \frac{RT}{\sqrt{2}n^2F^2c_s\sqrt{D}} \qquad [5]$$

where n is the number of electrons, D the diffusion coefficient of SH^-, c_s the surface concentration of SH^-, F Faraday's constant, R the universal gas constant, and T the absolute temperature. The values of the Warburg coefficient (σ_W) are plotted in Figure 14 for the

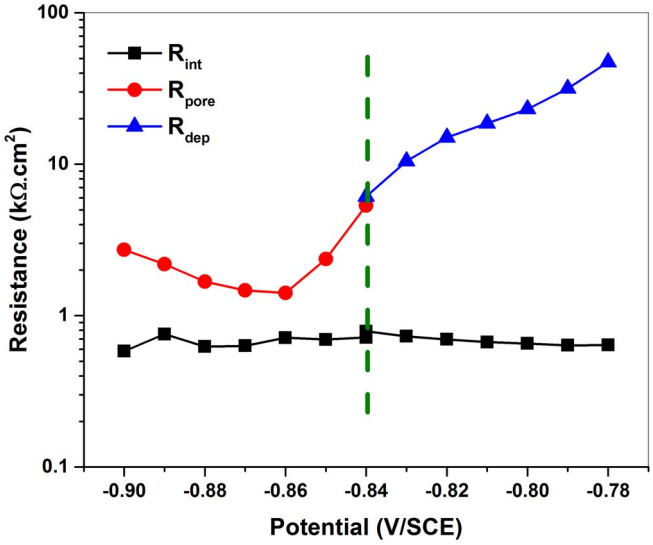

Figure 13. Resistance values obtained by fitting equivalent circuits in Figures 6b (−0.90 to −0.84 V/SCE) and 6d (−0.84 to −0.78 V/SCE) to EIS spectra recorded in a 0.1 M NaCl + 5 × 10^{-4} M Na_2S solution. The dotted line indicates the potential below which the equivalent circuit shown in Figure 6b was fit to the spectra and above which the equivalent circuit shown in Figure 6d was fit to the spectra. The two values at this potential show the fits of both equivalent circuits.

range of [SH^-] investigated. Reliable values could only be obtained up to potentials in the range −0.85 V/SCE to −0.84 V/SCE, except at the lowest [SH^-] for which a value was measurable up to ∼ −0.82 V/SCE.

Since σ_W is inversely proportional to c_S (Equation 5), the [SH^-] at the Cu surface, its value was expected to increase, as observed, as the potential was increased and SH^- became depleted at the base of the pores in the growing sulfide film. The similarity in σ_W values recorded at the various [SH^-] can be attributed to two counterbalancing influences: (i) an increase in the bulk solution [SH^-] which would increase the diffusive flux to maintain c_s; and (ii) an increase in film thickness which would increase the diffusion path length, leading to a decrease in c_s. At the lowest [SH^-], depletion was partially offset at low potentials by the increased porosity (decreased R_{pore}), Figure 10. Eventually, the ability to observe a transport contribution was lost when the film porosity increased more rapidly (at ∼−0.82 V/SCE, Figure 10), leading to an increase in c_S, and an increase in the interfacial oxidation rate (decrease in R_{int}), and the accumulation of the outer layer deposit (indicated by the high R_{dep} values).

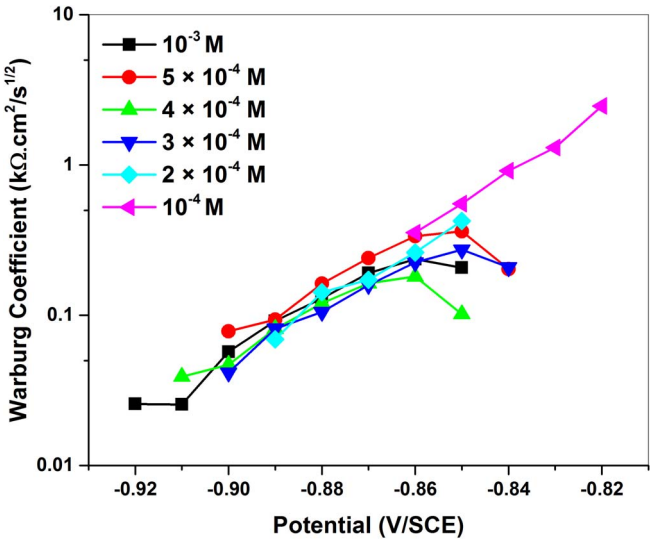

Figure 14. Warburg coefficients obtained from fitting the equivalent circuit shown in Figure 6b to EIS spectra.

At higher [SH^-], similar increases in σ_W, indicating decreased values of c_S, were observed at low potentials, Figure 14, confirming a contribution from SH^- transport to the film growth process, as indicated by the RDE experiments, Figure 3. However, in the potential region in which the current decreased markedly in the polarization curve (−0.86 V/SCE to −0.85 V/SCE, Figure 2), σ_W began to decrease, indicating an increase in c_S. This behavior confirmed our claim (above) based on the polarization curves (Figure 2) that the current peak which occurred in this potential range involved a restructuring of the film, leading to an increased porosity. The resulting increase in c_S would then account for the decrease in R_{int} at intermediate [SH^-] (Figure 11) and the maintenance of a low value at high [SH^-] (Figure 13). These observations confirm that this transition did not involve the formation of a passive film which would, by definition, have involved either an increase in R_{int} or an inability to observe the interfacial reaction. At these intermediate and high [SH^-], the high R_{dep} values then confirm that it is the rapid accumulation of the outer deposit which was responsible for the decrease in current, not the formation of a passive barrier layer.

These results confirm the importance of transport processes in determining the properties (morphology and porosity) of the Cu_2S film formed. In a previous voltammetric study[7] we showed that a protective sulfide film could be formed at a sufficiently high [SH^-] (∼10^{-3} M) under voltammetric conditions, provided the flux of SH^- to the Cu surface was maintained by convective flow (in that case, controlled by the use of a RDE). A similar dependence on convective flow, required to maintain the surface [SH^-], was observed under corrosion conditions.[24,25] Experiments performed under stagnant conditions demonstrated that Cu_2S film growth was controlled by SH^- diffusion in solution, leading to the formation of a non-protective film. By contrast, when SH^- transport was accelerated by convection, film growth rapidly became controlled by Cu^+ transport through a coherent film and proceeded at a considerably lower rate. This study, conducted under stagnant conditions in which the surface [SH^-] became depleted, confirmed that the films formed both electrochemically and by corrosion[24,25] are porous and not passive. Whether or not CuS is formed remains unresolved.

Conclusions

- The properties of copper sulfide films grown electrochemically on Cu in chloride solutions containing various amounts of sulfide (from 10^{-4} M to 10^{-3} M) have been investigated electrochemically.
- Film growth occurred in two distinct stages. At low positive potentials a thin porous Cu_2S film was formed, with growth occurring at the Cu_2S/electrolyte interface supported by the transport of Cu^+. This was followed by the deposition of a thicker outer layer of Cu_2S. At sufficiently high [SH^-], this led to partial blockage of the film growth process, with the overall film growth rate being controlled by the properties of this outer-layer deposit.
- EIS measurements confirmed that the decrease in the film growth rate at higher potentials and [SH^-] was due to the formation of this deposit, not to passivation of the surface by a coherent sulfide film.
- The film growth mechanisms under electrochemical and corrosion conditions were found to be very similar. These results confirm previous claims that the formation of a passive sulfide film will only be possible at high [SH^-] and SH^- flux. When a compacted bentonite buffer is present on the surface of a Cu container in a DGR these conditions will be unachievable, and passivation of waste container surfaces should not occur.

Acknowledgments

This research was funded by the Swedish Nuclear Fuel and Waste Management Company AB (SKB, Solna, Sweden), Posiva Oy (Olkiluoto, Finland) and the Nuclear Waste Management Organization (Toronto, Canada).

ORCID

T. Martino https://orcid.org/0000-0003-4710-968X
J. Chen https://orcid.org/0000-0003-4021-7127
J. J. Noël https://orcid.org/0000-0003-3467-4778

References

1. D. W. Shoesmith, "Assessing the corrosion performance of high-level nuclear waste containers," *Corrosion*, **62**, 703 (2006).
2. F. King, C. Lilja, K. Pedersen, P. Pitkänen, and M. Vähänen, *An update of the state-of-the-art report on the corrosion of copper under expected conditions in a deep geologic repository*, Technical report for Swedish Nuclear Fuel and Waste Management Company: TR-10-67, 2010.
3. F. King, C. Lilja, and M. Vähänen, "Progress in the understanding of the long-term corrosion behaviour of copper canisters," *J. Nucl. Mater.*, **438**, 228 (2013).
4. F. King, *Corrosion of copper in alkaline chloride environments*, Technical report for Swedish Nuclear Fuel and Waste Management Company: TR-02-25, 2002.
5. R. Sandström and H. C. M. Andersson, "The effect of phosphorus on creep in copper," *J. Nucl. Mater.*, **372**, 66 (2008).
6. J. Chen, Z. Qin, and D. W. Shoesmith, "Kinetics of Corrosion Film Growth on Copper in Neutral Chloride Solutions Containing Small Concentrations of Sulphide," *J. Electrochem. Soc.*, **157**, C338 (2010).
7. T. Martino, R. Partovi-Nia, J. Chen, Z. Qin, and D. W. Shoesmith, "Mechanisms of Film Growth on Copper in Aqueous Solutions Containing Sulphide and Chloride under Voltammetric Conditions," *Electrochim. Acta.*, **127**, 439 (2014).
8. T. Martino, J. Chen, Z. Qin, and D. W. Shoesmith, "The kinetics of film growth and their influence on the susceptibility to pitting of copper in aqueous sulphide solutions," *Corros. Eng. Sci. Technol.*, **52**, 61 (2017).
9. M. R. Gennero De Chialvo and A. J. Arvia, "The electrochemical behaviour of copper in alkaline solutions containing sodium sulphide," *J. Appl. Electrochem.*, **15**, 685 (1985).
10. J. Chen, Z. Qin, and D. W. Shoesmith, "Long-term corrosion of copper in a dilute anaerobic sulphide solution," *Electrochim. Acta.*, **56**, 7854 (2011).
11. J. Chen, Z. Qin, and D. W. Shoesmith, "Rate controlling reactions for copper corrosion in anaerobic aqueous sulphide solutions," *Corros. Eng. Sci. Technol.*, **46**, 138 (2011).
12. J. Chen, Z. Qin, and D. W. Shoesmith, "Copper Corrosion in Aqueous Sulphide Solutions under Nuclear Waste Repository Conditions. in *Mater. Res. Soc. Symp. Proc.* 2012.
13. J. Chen, Z. Qin, T. Martino, and D. W. Shoesmith, "Non-uniform film growth and micro/macro-galvanic corrosion of copper in aqueous sulphide solutions containing chloride," *Corros. Sci.*, **114**, 72 (2017).
14. J. Chen, Z. Qin, T. Martino, and D. W. Shoesmith, "Effect of chloride on Cu corrosion in anaerobic sulphide solutions," *Corros. Eng. Sci. Technol.*, **52**, 40 (2017).
15. F. King, D. S. Hall, and P. G. Keech, "Nature of the near-field environment in a deep geological repository and the implications for the corrosion behaviour of the container," *Corros. Eng. Sci. Technol.*, **52**, 25 (2017).
16. C. F. Dong, F. X. Mao, S. J. Gao, S. Sharifi-Asl, P. Lu, and D. D. Macdonald, "Passivity Breakdown on Copper: Influence of Temperature," *J. Electrochem. Soc.*, **163**, C707 (2016).
17. D. Kong, C. Dong, A. Xu, C. Man, C. He, and X. G. Li, "Effect of Sulphide Concentration on Copper Corrosion in Anoxic Chloride-Containing Solutions," *J. Mater. Eng. Perform.*, **26**, 1741 (2017).
18. D. C. Kong, C. F. Dong, X. Q. Ni, A. N. Xu, C. He, K. Xiao, and X. G. Li, "Long-term polarisation and immersion for copper corrosion in high-level nuclear waste environment," *Mater. Corros.*, **68**, 1070 (2017).
19. S. Cassaignon, S. Sanchez, J.-F. Guillemoles, J. Vedel, and H. Gomez Meier, "Influence of the Composition on the Copper Diffusion in Copper Sulphides Study by Impedance Spectroscopy," *J. Electrochem. Soc.*, **146**, 4666 (1999).
20. B. Zhang, S. Hao, J. Wu, X. Li, and Y. Huang, "Evidence of a nanosized copper anodic reaction in an anaerobic sulphide aqueous solution," *RSC Adv.*, **6**, 19937 (2016).
21. J. M. Smith, "The corrosion and electrochemistry of copper in aqueous, anoxic sulphide solutions," Ph.D. Thesis, Western University (2007).
22. E. Barsoukov and J.R. Macdonald, (eds.), *Impedance Spectroscopy: Theory, Experiment, and Applications*, 2nd edn.,Wiley, 2005.
23. C. H. Hsu and F. Mansfeld, "Technical Note: Concerning the Conversion of the Constant Phase Element Parameter Y0 into a Capacitance. *Corrosion.*, **57**, 747 (2001).
24. J. Chen, Z. Qin, and D. W. Shoesmith, "Key parameters determining structure and properties of sulphide films formed on copper corroding in anoxic sulphide solutions," *Corros. Eng. Sci. Technol.*, **49**, 415 (2014).
25. J. Chen, Z. Qin, L. Wu, J. J. Noel, and D. W. Shoesmith, "The influence of sulphide transport on the growth and properties of copper sulphide films on copper," *Corros. Sci.*, **87**, 233 (2014).